Cell

PIDD Mediates NF-κB Activation in Response to DNA Damage

Sophie Janssens,[1,2] Antoine Tinel,[1,2] Saskia Lippens,[1] and Jürg Tschopp[1,*]
[1] Department of Biochemistry, University of Lausanne, BIL Biomedical Research Center, Chemin des Boveresses 155, CH-1066 Epalinges, Switzerland
[2] These authors contributed equally to this work.
*Contact: jurg.tschopp@unil.ch
DOI 10.1016/j.cell.2005.09.036

SUMMARY

Activation of NF-κB following genotoxic stress allows time for DNA-damage repair and ensures cell survival accounting for acquired chemoresistance, an impediment to effective cancer therapy. Despite this clinical relevance, little is known about pathways that enable genotoxic-stress-induced NF-κB induction. Previously, we reported a role for the p53-inducible death-domain-containing protein, PIDD, in caspase-2 activation and apoptosis in response to DNA damage. We now demonstrate that PIDD plays a critical role in DNA-damage-induced NF-κB activation. Upon genotoxic stress, a complex between PIDD, the kinase RIP1, and a component of the NF-κB-activating kinase complex, NEMO, is formed. PIDD expression enhances genotoxic-stress-induced NF-κB activation through augmented sumoylation and ubiquitination of NEMO. Depletion of PIDD and RIP1, but not caspase-2, abrogates DNA-damage-induced NEMO modification and NF-κB activation. We propose that PIDD acts as a molecular switch, controlling the balance between life and death upon DNA damage.

INTRODUCTION

Although the transcription factor NF-κB is mainly associated with its pivotal role in immune and inflammatory responses, it has been known for a long time that NF-κB is also induced by ''noninflammatory'' activators such as oxidative or genotoxic stress (Pahl, 1999). Indeed, DNA-damage-induced NF-κB activation controls the transcription of cell survival genes, allowing cells to escape the otherwise lethal effect of DNA damage and to initiate pathways of DNA repair. In this regard, activation of NF-κB by chemotherapeutic compounds accounts for the phenomenon of acquired chemoresistance that impedes effective cancer therapy (Baldwin, 2001). Despite this notable clinical relevance, little is known about the pathways enabling genotoxic-stress-induced NF-κB induction.

NF-κB is a dimeric transcription factor composed of members of the Rel family, the most abundant dimer in the cell being RelA/p50 (for a recent review, see Hayden and Ghosh, 2004). In unstimulated cells, NF-κB is sequestered in the cytoplasm through interaction with an inhibitory protein, IκB, which masks its nuclear localization signal. Almost all activators of NF-κB converge on the release of IκB through activation of an IκB kinase (IKK) complex that induces IκB phosphorylation. This targets IκB for ubiquitination and subsequent degradation, allowing freed NF-κB to translocate to the nucleus and activate transcription of target genes. The IKK complex is composed of two related kinases, IKKα and IKKβ, and a regulatory scaffolding subunit, NEMO (alternatively called IKKγ). During the past years, numerous groups have contributed to our understanding of cell-surface-receptor-induced NF-κB activation, unraveling for example the main signaling pathways emanating from the tumor necrosis factor (TNF) receptor family or the interleukin-1/Toll-like receptor (TLR) family (Bonizzi and Karin, 2004).

Far less understood are the so-called ''nuclear-to-cytoplasmic'' pathways that trigger NF-κB activation, such as those activated by DNA damage. The nature of the signaling cascade initiated appears to depend strongly on the genotoxic stimulus and cell type used as well as on dose and timing of the stimulus, giving rise to many discrepancies in the literature and hindering the emergence of a general model. In spite of this, some of the key events have been identified. With the exception of UV irradiation, which appears to induce an entirely unrelated pathway (Kato et al., 2003), most DNA-damage-inducing signals converge at the level of the phosphorylation of cytoplasmic IκB through activation of the IKK complex, similar to the classical activation of NF-κB (e.g., (Huang et al., 2000; Hur et al., 2003)). The activation of the IKK complex in response to irradiation or topoisomerase I- or II-targeting drugs is strictly dependent on the presence of the nucleus and the formation of double strand breaks, showing the intimate link between the presence of DNA lesions and NF-κB activation and suggesting that

NF-κB activation forms part of a general cellular response induced upon DNA damage (Boland et al., 2000; Huang et al., 2000). A central component of the DNA-damage response is the PI3-like kinase ATM (for *a*taxia *t*elangiectasia *m*utated) that is rapidly phosphorylated upon DNA double-strand break (DSB) formation and in this way acts as a sensor of chromatin alterations. ATM mounts a decisive, meticulously orchestrated response through phosphorylation of several key targets implicated in cell cycle control, DNA repair or stress responses (for a review see Shiloh, 2003). ATM-deficient cells from patients with the genomic instability disorder ataxia telangiectasia are no longer able to activate NF-κB in response to ionizing irradiation or treatment with the topoisomerase I poison camptothecin (CPT), indicating that ATM also plays a pivotal role in activation of NF-κB (Li et al., 2001; Piret et al., 1999). Supposedly, ATM directly phosphorylates IκB, based on in vitro assays (Jung et al., 1997), but this has never been confirmed in vivo and, until recently, ATM's target substrate in the NF-κB pathway remained obscure.

A major breakthrough was recently provided by the group of Miyamoto (Huang et al., 2003), who demonstrated that ATM is needed for ubiquitination of NEMO. In response to DNA damage, NEMO appears to translocate to the nucleus and undergo a series of posttranslational modifications (subsequently sumoylation, phosphorylation, and ubiquitination), which allows NEMO to be activated and be released from the nucleus again, providing a means to link nuclear DNA damage to the activation of the cytoplasmic IKK complex. ATM is not needed for NEMO sumoylation, however, leaving the initial signal leading to nuclear translocation of NEMO and its SUMO modification unidentified.

Sumoylation or the posttranslational modification of proteins through covalent attachment with the small ubiquitin-related protein SUMO is emerging as an important regulatory mechanism that affects protein function through altered interaction properties, retargeting of modified proteins to specific subcellular compartments, or by antagonizing other modifications that occur at the same lysine (Hay, 2005; Seeler and Dejean, 2003). Sumoylation occurs in a way that is highly analogous to ubiquitination. Four subsequent enzymatic reactions lead to the maturation of SUMO; its activation through linkage via a thioesther bond with the E1 enzyme UBA2/Aos; its conjugation to the E2 enzyme Ubc9; and, finally, its ligation to its target, which might occur in an E3-independent way or by means of E3 ligases such as members of the PIAS (protein inhibitor of activated STATs) family, RanBP2, or polycomb protein Pc2 (Johnson and Gupta, 2001; Kagey et al., 2003; Pichler et al., 2002).

Reminiscent of the caspase-9 apoptosome complex, caspase-2 has been shown to form a high-molecular-weight complex in cell extracts, albeit independently from Apaf or cytochrome c (Read et al., 2002). We demonstrated previously that recruitment and activation of caspase-2 within this complex is entirely dependent on the presence of RAIDD and the p53-inducible protein PIDD, which together with caspase-2 constitute the so-called PIDDosome (Tinel and Tschopp, 2004). PIDD contains a C-terminal death domain (DD) through which it recruits RAIDD; N-terminal leucine-rich repeats (LRRs), probably involved in the recognition of a stress-related signal of unknown nature; and two internal ZU5 domains, which, together with the region in between the ZU5 and the DD, are most likely implicated in PIDD oligomerization. Although the full-length protein has a molecular mass of approximately 100 kDa, both endogenous and overexpressed PIDD are constitutively processed at two sites, giving rise to a 48 kDa N-terminal fragment and a C-terminal fragment of 51 kDa, which is further cleaved, resulting in a 37 kDa fragment (Telliez et al., 2000; Tinel and Tschopp, 2004).

Activation of the PIDDosome sensitizes cells to genotoxic-stress-induced apoptosis (Tinel and Tschopp, 2004). In addition to DNA damage, however, lysis of cells under hypotonic conditions can also initiate assembly of the PIDDosome. In the present work, we observed that PIDD interacts with NEMO and RIP1 under these in vitro conditions, motivating us to investigate whether the PIDDosome might be implicated in the activation of NF-κB as well. We will demonstrate a critical role for PIDD in DNA-damage-induced activation of NF-κB and, more specifically, in the pathway leading to SUMO modification of NEMO.

RESULTS

The PIDDosome Incorporates NF-κB Signaling Components

Assembly and activation of the PIDDosome can be initiated in vitro by lysing PIDD-expressing cells under hypotonic conditions at 4ºC, followed by incubation at 37ºC. This results in the recruitment of caspase-2 to PIDD via RAIDD (Figure 1; Tinel and Tschopp, 2004). In order to further dissect the composition of the PIDDosome, we analyzed the complex for the possible presence of another death-domain protein, RIP1, which has been linked previously to genotoxic-stress-induced signaling (Hur et al., 2003). The RIP1 kinase is a crucial component of several signaling pathways that activate NF-κB, such as those emanating from TNF receptors (TNF-R) or TLR3 (Meylan and Tschopp, 2005), and can bind directly to NEMO (Hayden and Ghosh, 2004). Immunoprecipitation of PIDD after different periods of activation at 37ºC revealed that RIP1 and also NEMO were recruited to the PIDDosome in a stimulus-dependent manner (Figure 1). In contrast, two other known NF-κB intermediates, the RIP1-related protein RIP2 and TRAF6, were not present in the PIDDosome, confirming the specificity of the PIDD-RIP1-NEMO interaction.

PIDD Is Necessary but Not Sufficient for DNA-Damage-Induced NF-κB Activation

The above-mentioned results prompted us to investigate whether the PIDDosome might be implicated in the activation of NF-κB. In contrast to RIP1, transient overexpression of PIDD or RAIDD in HEK293T cells was not sufficient to induce NF-κB activation, as measured by an NF-κB-dependent reporter gene assay (Figure 2A). We previously noticed that assembly of the PIDDosome is also not sufficient to induce apoptosis but that a second signal (i.e., DNA damage) is required for full commitment to caspase-2-mediated cell death (Tinel and Tschopp, 2004). Hence, we tested whether

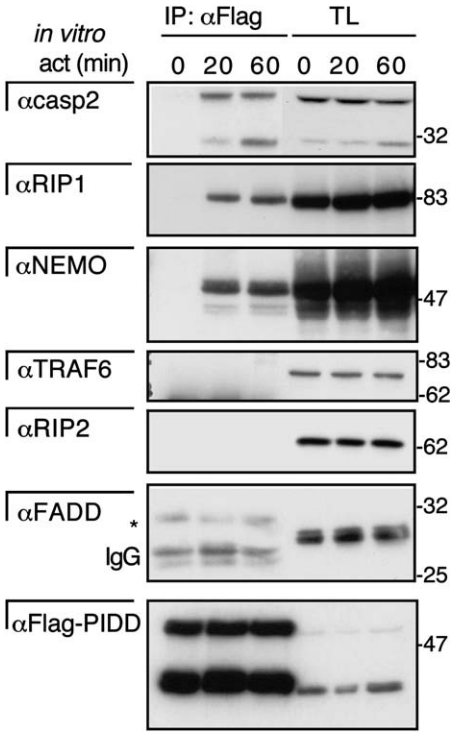

Figure 1. The PIDDosome Incorporates NF-κB Signaling Components

HEK293T cells stably expressing Flag-PIDD were lysed under hypotonic conditions and incubated for the indicated times at 37°C to allow spontaneous formation of the PIDDosome complex. Anti-Flag-PIDD immunoprecipitates were analyzed for the presence of caspase-2, RIP1, NEMO, TRAF6, RIP2, FADD, and Flag-PIDD by Western blot. *represents an unspecific band recognized by the FADD antibody. IP, immunoprecipitates; TL, total cell lysate.

cells stably expressing PIDD were sensitized for genotoxic-stress-induced NF-κB activation. To this end, we tested topoisomerase I (CPT) as well as topoisomerase II (doxorubicin [dox] and etoposide [eto]) targeting poisons. Although they all lead to the formation of double-strand breaks and, concomitantly, activation of ATM (Avemann et al., 1988; Bromberg et al., 2003; Tewey et al., 1984), they can induce different NF-κB responses. While particularly etoposide is known to activate NF-κB transcriptional responses, doxorubicin is known to be a weak inducer of NF-κB transcriptional activity and might in certain cell types even lead to a repression of NF-κB-dependent gene transcription (Campbell et al., 2004; Huang et al., 2000). However, its potential to activate the NF-κB pathway can easily be demonstrated at the level of IκB phosphorylation or NF-κB DNA binding. As can be seen in Figure 2B and Figure S1A in the Supplemental Data available with this article online, HEK293T cells stably expressing PIDD showed enhanced NF-κB transcriptional activation upon stimulation with these different genotoxic agents. This increased activation of the NF-κB signaling cascade was also detected at the level of IκB phosphorylation (Figure 2C; see also below). In comparison with mock-transfected cells, cells stably expressing PIDD showed a slightly increased basal phosphorylation of IκB, and maximal levels of IκB phosphorylation upon etoposide treatment were reached more rapidly. The stimulating effect of PIDD on the NF-κB pathway was not restricted to HEK293T cells but was also observed in HeLa cells that had been stimulated with either etoposide or doxorubicin (Figure S1B). Furthermore, knockdown of endogenous PIDD levels in HEK293T cells through the use of siRNA led to a substantial inhibition of etoposide-induced phosphorylation of IκB (Figure 2D and Figure 3C) and impaired NF-κB DNA binding (Figure 2E and Figure S1E). As a result, we could not detect an augmentation of Bcl-xL or XIAP mRNA, which are both known to be NF-κB target genes (Figure 2F). The inhibitory effect of PIDD siRNA treatment on NF-κB activation was also observed in other cell types, such as U2OS cells (see below), or with other genotoxic agents, such as CPT or doxorubicin (see below and Figure S1C). Importantly, knockdown of PIDD expression did not cause a general block in the DNA-damage response as ATM was still phosphorylated upon etoposide stimulation (Figure S1D). Taken together, these results identify PIDD as a crucial component of the genotoxic-stress-triggered signaling pathway that leads to NF-κB activation.

PIDD Causes Modification of NEMO

To further investigate how PIDD might be implicated in genotoxic stress signaling, we analyzed endogenous NEMO protein modifications induced by DNA damage. Confirming previous results (Huang et al., 2003), we found that NEMO became sumoylated in a time-dependent manner in response to etoposide or doxorubicin (Figure 3A, left panel). However, the amount of modified NEMO was marginal, which correlates with the data of Huang that causes these authors and others to speculate that NEMO is rapidly desumoylated once it is recognized by the ATM scaffold (Hay, 2004; Huang et al., 2003). Quite strikingly, the modified form of NEMO was much more apparent in PIDD-expressing cells than in mock cells (Figure 3A, right panel). To prove that this modification was indeed a sumoylated form of NEMO, we prepared lysates of nontreated, TNF-, or etoposide-treated mock and PIDD-expressing cells; immunoprecipitated NEMO under conditions designed to prevent association with other interacting proteins; and monitored SUMO-1 (hereafter called SUMO) modification (Figure 3B). In PIDD-expressing cells, endogenous SUMO-modified NEMO was readily detected upon genotoxic stress but not upon TNF stimulation. These experiments therefore indicate a role for PIDD in the initial modification step of NEMO. Again in agreement with the data of Huang et al., NEMO was not only sumoylated but also ubiquitinated. Ubiquitination of NEMO upon DNA damage was more readily detectable in PIDD-expressing cells compared to mock cells (Figure 3B). This is not surprising as sumoylation of NEMO appears to be a prerequisite for its subsequent ubiquitination (Huang et al., 2003).

There is accumulating evidence that NEMO is polyubiquitinated in response to different stimuli, inducing the activation of the IKKs rather than its proteasome-mediated degradation (Burns and Martinon, 2004). Intriguingly, different

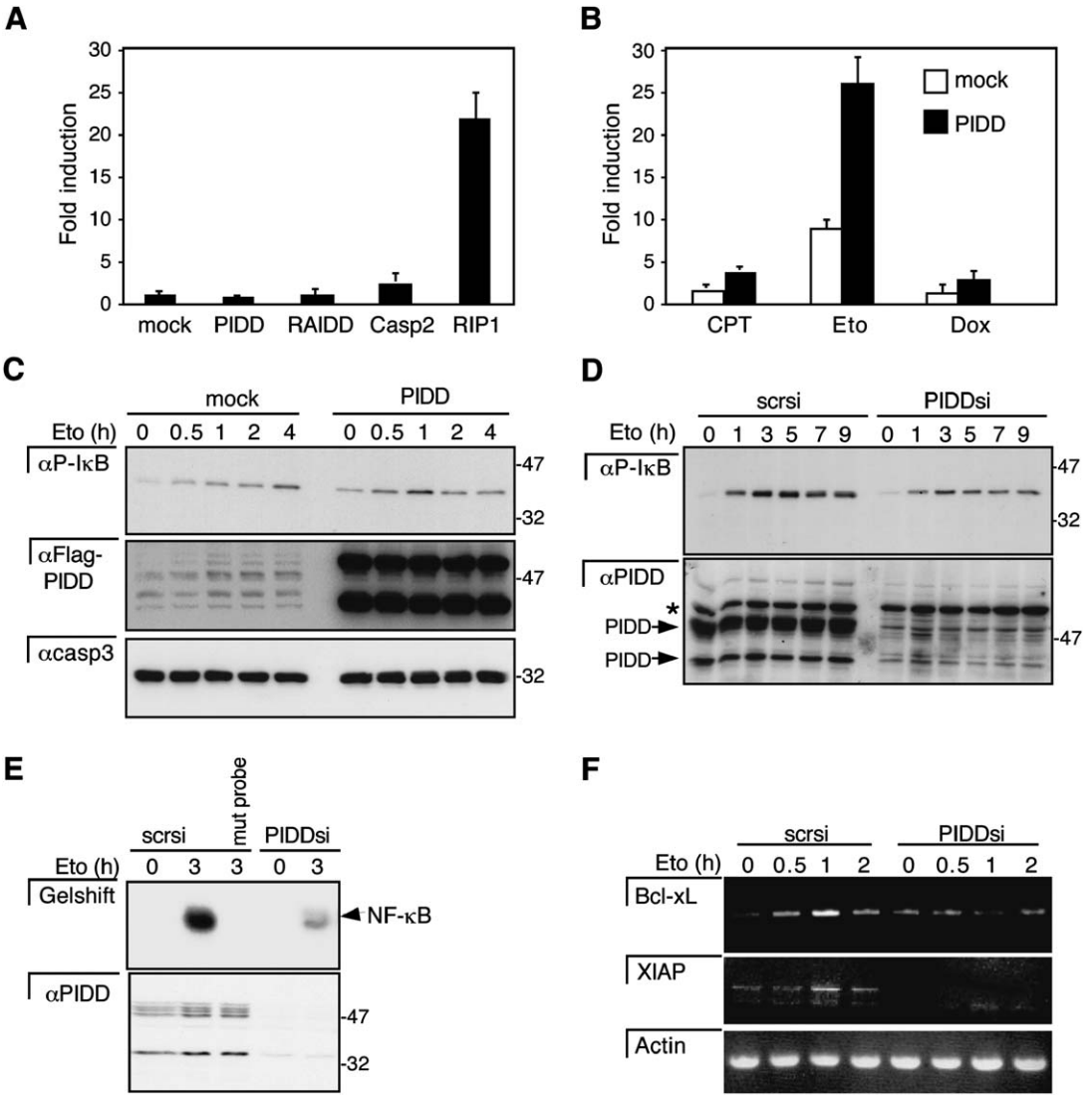

Figure 2. PIDD Is Necessary but Not Sufficient for DNA-Damage-Induced NF-κB Activation

(A) Overexpression of PIDD does not induce NF-κB activation. HEK293T cells were transiently transfected with expression vectors encoding PIDD, RAIDD, caspase-2, or RIP1 combined with an NF-κB-dependent luciferase reporter gene and a β-galactosidase internal reporter. Luciferase activity in cell extracts was normalized for differences in transfection efficiency on the basis of β-galactosidase activity. Values are the mean (± standard deviation) of three different transfections and are expressed as fold induction relative to the mock (empty vector) control.

(B) HEK293T cells stably expressing PIDD are sensitized for DNA-damage-induced NF-κB activation. Mock-transfected cells (white bars) or PIDD-expressing cells (black bars) were stimulated for 16 hr with 50 μM CPT, 40 μM etoposide (Eto), or 2 μg/ml doxorubicin (Dox). NF-κB activation was evaluated using the luciferase reporter gene assay. Values are the mean (± standard deviation) of three different transfections and are expressed as fold induction relative to unstimulated cells.

(C) Etoposide-induced phosphorylation of IκB occurs faster and reaches higher maximal levels in PIDD stable cells. Mock-transfected cells or PIDD-expressing cells were stimulated for the indicated times with 40 μM etoposide, lysed, and analyzed for phospho-IκB and Flag-PIDD levels. Caspase-3 was used as a loading control.

(D) siRNA against PIDD blocks genotoxic-stress-induced NF-κB activation. HEK293T cells were transfected with siRNA constructs for PIDD or a scrambled control. Forty-eight hours after transfection, cells were stimulated for the indicated times with 40 μM etoposide and analyzed for phospho-IκB and PIDD levels by Western blot. *represents an unspecific band, recognized by the mouse secondary antibody, which demonstrates equal loading.

(E) siRNA against PIDD abrogates etoposide-induced NF-κB DNA binding. HEK293T cells were transfected with siRNA for PIDD or a scrambled control. Forty-eight hours after transfection, cells were stimulated for three hours with 40 μM etoposide and analyzed for NF-κB DNA binding by an EMSA (gel shift) assay. In the third lane, a control reaction is shown in which we incubated a lysate of an etoposide-treated sample with a mutant NF-κB probe. Cytosolic extracts were verified for PIDD expression.

(F) siRNA against PIDD blocks etoposide-induced expression of NF-κB-dependent genes. U2OS cells were transfected with siRNA constructs targeting PIDD or a scrambled control. Forty-eight hours after transfection, cells were stimulated for the indicated times with 40 μM etoposide and analyzed for the expression levels of Bcl-xL, XIAP, and actin mRNA by RT-PCR.

agents induce different ubiquitin profiles, most likely providing a means for NEMO to integrate various responses via the recruitment of specific ubiquitin binding proteins. TNF is one of the agents that induce NEMO ubiquitination. However, we could not detect any augmentation of the TNF-induced NEMO ubiquitin signal in PIDD-expressing cells (Figure 3B), arguing against a general role for PIDD in NEMO modification. We next checked whether knockdown of PIDD interfered with genotoxic-stress-induced NEMO modification. As can be seen in Figure 3C, siRNA against PIDD abrogated etoposide- and doxorubicin-induced sumoylation of NEMO, leading to a reduction in genotoxic-stress-induced phosphorylation of NEMO, which is thought to be induced in a subsequent step, through the action of ATM (Huang et al., 2003). Concomitantly, phosphorylation of IκB was impaired in PIDD siRNA-treated cells. SiRNA treatment against RAIDD did not have such effects. Rather, genotoxic-stress-induced modifications of NEMO appeared to be slightly enhanced, leading to a stronger induction of phospho-IκB (see also later). Finally, we immunoprecipitated NEMO in conditions preventing association with other proteins to evaluate sumoylation and ubiquitination of NEMO (Figure 3D). In keeping with the data from Figure 3B, we only detected very faint SUMO signals under these conditions (which again appeared to be less in PIDD siRNA-treated cells; data not shown), while we could easily observe a strong inhibitory effect of PIDD siRNA on doxorubicin-induced ubiquitination of NEMO. In conclusion, downregulation of endogenous PIDD levels leads to a strong inhibition of NEMO sumoylation, phosphorylation, and ubiquitination in response to genotoxic stress, thus explaining the impaired NF-κB response.

RIP1 Is Required for the Recruitment of NEMO to PIDD

PIDD interacts not only with the NF-κB signaling intermediate NEMO but also with RIP1 upon in vitro PIDDosome activation (see Figure 1). Interestingly, RIP1 was previously shown to be essential for genotoxic-stress-induced signaling to NF-κB (Hur et al., 2003), although its exact function and/or position in the pathway remained unclear. We therefore generated Jurkat cells derived from either RIP1-wt or RIP1-deficient clones that stably express PIDD. Subsequent to genotoxic stress or TNF stimulation, endogenous NEMO was immunoprecipitated under stringent conditions to prevent association with other interacting proteins. Sumoylation and ubiquitination of NEMO were only detectable in cells expressing PIDD derived from RIP1-wt but not from RIP1-deficient cells (Figure 4A), and this only upon genotoxic stress. Confirming our previous results (Figure 3), the increased sumoylation and ubiquitination of NEMO correlated with a strongly enhanced activation of the NF-κB pathway (Figure 4A).

To further characterize the role of RIP1 in PIDD-induced sumoylation of NEMO, we analyzed in vitro PIDDosome complex formation in lysates prepared from RIP1-wt or RIP1-deficient PIDD-expressing Jurkat cells. NEMO recruitment to PIDD was only detected in RIP1-wt but not in RIP1-deficient cells, indicating that RIP1 mediates the interaction of PIDD with NEMO (Figure 4B). Interestingly, more RAIDD and caspase-2 were recruited to PIDD in RIP1-deficient cells (Figure 4B). Moreover, caspase-2 cleavage was much more apparent in RIP1-deficient cells, suggesting a hyperactivation of the PIDD-RAIDD-caspase-2 pathway in the absence of RIP1.

The PIDD-RIP1-NEMO complex was not only formed in vitro but also assembled in PIDD-expressing cells upon genotoxic stress (Figure 4C). Interestingly, preferentially SUMO-modified NEMO was detected in the assembling PIDDosome, while the unmodified form of NEMO was barely discernible in PIDD immunoprecipitates. This is in contrast to the in vitro assay, where only the 47 kDa unmodified form of NEMO was detected (Figure 4B), indicating that incubation of hypotonic lysates at 37°C is sufficient to trigger PIDDosome formation but not NEMO modification. This is in keeping with the observation that phosphorylation of IκB is not detectable in the in vitro assembly assay (Figure 4B, lower panel). Thus, the mere formation of a complex between PIDD, RIP1, and NEMO is not sufficient to induce NEMO sumoylation and the subsequent activation of NF-κB.

PIDD Shuttles to the Nucleus in Response to Genotoxic Stress

In unstimulated cells, PIDD was localized predominantly in the cytoplasm (Figure 5A). However, when cells were treated with leptomycin B, a known inhibitor of the nuclear export protein CRM1 (Fukuda et al., 1997), PIDD accumulated in the nucleus, demonstrating that PIDD can shuttle between cytosol and nucleus (Figure 5A). Genotoxic stimuli such as CPT and doxorubicin, but not TNF, also led to nuclear accumulation of a small portion of PIDD (Figure 5B and Figure S2). Biochemical fractionation experiments yielded similar results. Upon genotoxic stress, cytosolic PIDD levels declined, while nuclear PIDD levels increased (Figure 5C). In contrast, we could not detect any translocation of RIP1 or NEMO to the nucleus. As is apparent from Figure 5C, a substantial portion of both RIP1 and NEMO was already present in the nucleus in unstimulated cells, and the ratio between nuclear and cytoplasmic levels was unaffected upon induction of DNA damage. Of note, genotoxic-stress-induced sumoylation of NEMO was only detected in the nucleus. Additionally, we observed that the nuclear fraction of NEMO exhibited a slightly higher molecular mass and migrated as a doublet. This modification was independent of the genotoxic stress signals applied. Interestingly, the other PIDD-interacting protein, RIP1, was also modified exclusively in the nuclear fraction. While the nature of this modification is currently not known, these results show that, upon genotoxic stress, a portion of PIDD accumulates in the nucleus where modification of RIP1 and NEMO is observed.

PIDD-Induced NF-κB and Apoptosis Pathways Are Independent

A role for caspase-2 in NF-κB activation was recently proposed (Lamkanfi et al., 2005). As shown in Figure 2A, we also consistently observed a small NF-κB activating potential mediated by caspase-2 upon overexpression in cells. However, neither siRNA against endogenous caspase-2 nor siRNA against endogenous RAIDD affected

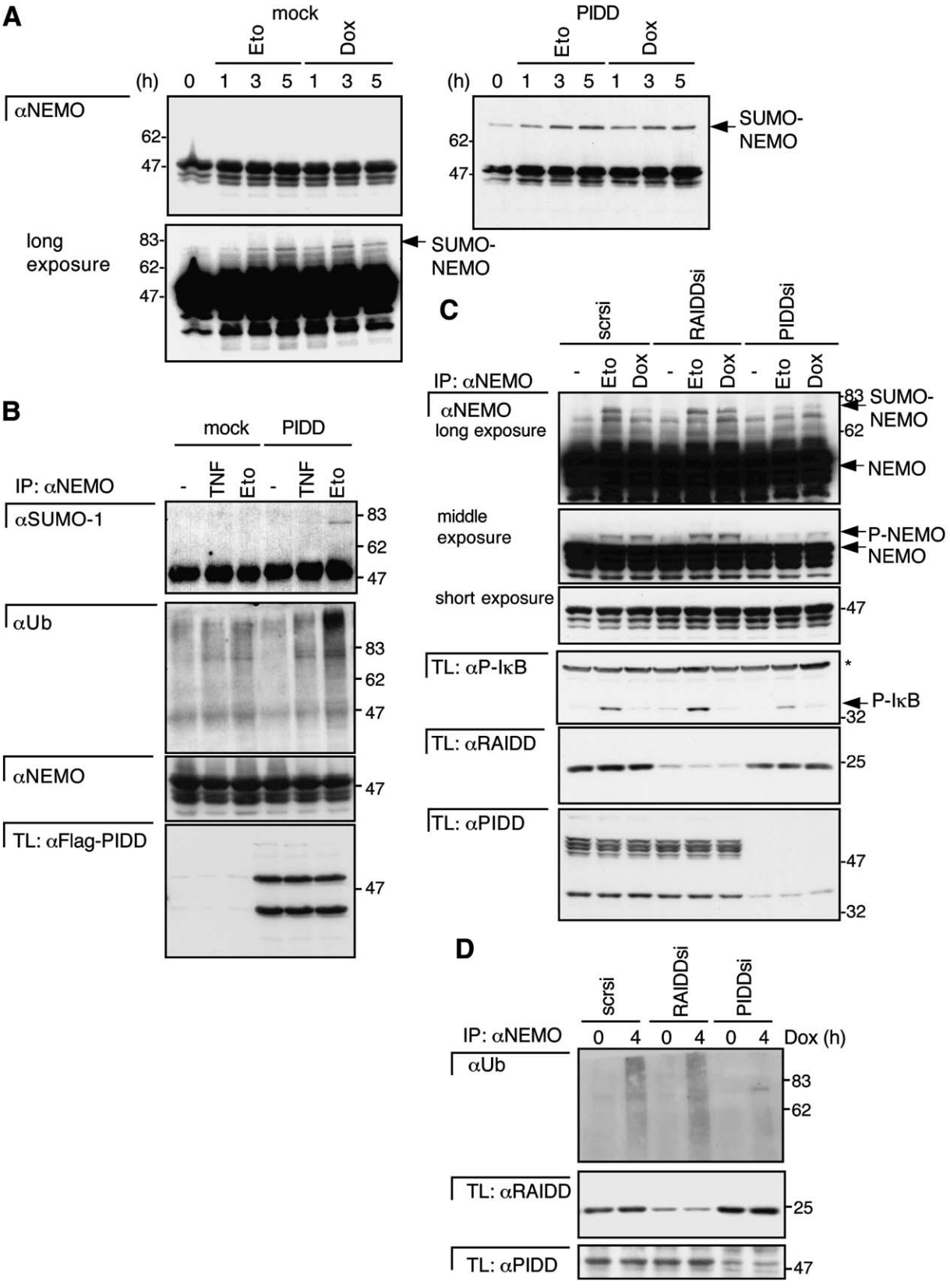
A
mock
PIDD
Eto
Dox
(h) 0 1 3 5 1 3 5
αNEMO
62-
47-
long exposure
83-
62-
47-
SUMO-NEMO
B
mock
PIDD
IP: αNEMO
- TNF Eto - TNF Eto
αSUMO-1
αUb
αNEMO
TL: αFlag-PIDD
83
62
47
C
scrsi
RAIDDsi
PIDDsi
- Eto Dox - Eto Dox - Eto Dox
IP: αNEMO
αNEMO long exposure
middle exposure
short exposure
SUMO-NEMO
NEMO
P-NEMO
TL: αP-IκB
P-IκB
TL: αRAIDD
TL: αPIDD
25
32
D
scrsi
RAIDDsi
PIDDsi
IP: αNEMO
0 4 0 4 0 4 Dox (h)
αUb
TL: αRAIDD
TL: αPIDD

genotoxic-stress-induced NF-κB activation (Figure 6A and Figure 3C), making a physiologically relevant role for caspase-2 or RAIDD in DNA-damage-induced activation of NF-κB unlikely. These data led us to envisage the possibility that PIDD acts as a docking platform, either interacting with a survival complex consisting of the NF-κB signaling proteins RIP1 and NEMO or interacting with a death-inducing complex consisting of RAIDD and caspase-2. To strengthen this hypothesis, we tested whether RIP1 and RAIDD could interact simultaneously with PIDD. Figure 6B shows that increasing amounts of RAIDD competed with RIP1 for binding to PIDD and vice versa, strongly suggesting that RAIDD and RIP1 interact in a mutually exclusive manner with PIDD. This is in agreement with data shown in Figure 4B, where, in RIP1-deficient cells, more RAIDD and caspase-2 were found to interact with PIDD upon in vitro formation of the PIDDosome. Furthermore, more caspase-2 was cleaved in the absence of RIP1 (Figure 4B), suggesting a hyperactivation of the PIDD-RAIDD-caspase-2 pathway. Alternatively, when RAIDD levels were downregulated by siRNA treatment (such as shown in Figure 3C), thereby blocking the PIDD proapoptotic pathway, genotoxic agents induced a stronger SUMO modification of NEMO, leading to an exacerbation of the PIDD NF-κB pathway. Finally, we analyzed in vitro PIDDosome assembly at early time points to possibly detect a difference in kinetics for RIP1 and RAIDD recruitment to PIDD. As can be seen in Figure 6C, RIP1 and NEMO were recruited almost immediately to PIDD, while RAIDD and caspase-2 were detectable only at later time points, suggesting a sequential recruitment of the two complexes.

DISCUSSION

The death-domain protein PIDD was originally identified as an early p53-inducible gene that is implicated in p53-induced apoptosis (Lin et al., 2000). Cells stably expressing PIDD are strongly sensitized for genotoxic-stress-induced apoptosis through the formation of a so-called PIDDosome, which contains the adaptor protein RAIDD and caspase-2 and triggers the mitochondrial pathway of apoptosis (Tinel and Tschopp, 2004). In the present study, we confirm the critical role for PIDD as a mediator of the DNA-damage-activated stress response and show its additional involvement in genotoxic-stress-induced NF-κB activation.

The signals that relay nuclear DNA damage to the activation of cytoplasmic IKK complex and thus NF-κB are still poorly defined. Only recently, Huang et al. discovered that posttranslational modifications of NEMO play a central role in this process (Huang et al., 2003). Two separate, parallel pathways are needed to permit NEMO modifications. A first pathway, induced by a so far unidentified signaling cascade, leads to NEMO sumoylation and, as a consequence, its nuclear retention, while a second, ATM-dependent pathway results in NEMO phosphorylation and subsequent ubiquitination. This allows NEMO to be released from the nucleus and to activate the cytoplasmic IKK complex (Hay, 2004; Huang et al., 2003). This two-way model is supported by the observation that artificial SUMO attachment to NEMO is not sufficient to induce NF-κB activation; neither is overexpression of ATM, showing the requirement of both signals.

In this study, we have identified PIDD as an essential component in the pathway that leads to DNA-damage-mediated NEMO sumoylation. Increased PIDD expression results in highly augmented levels of SUMO-modified NEMO, while knockdown of PIDD inhibits this posttranslational modification. As a consequence, NEMO phosphorylation and ubiquitination are also affected. Sumoylation of target proteins is frequently involved in the control of subcellular localization, and numerous recent reports demonstrate a close link between sumoylation and nuclear retention (Endter et al., 2001; Li et al., 2005; Rangasamy et al., 2000). This presumptive function of sumoylation appears to hold true for NEMO since artificial fusion of NEMO to SUMO is sufficient to induce its nuclear accumulation (Huang et al., 2003). NF-κB activation upon genotoxic stress occurs faster and is more persistent in the presence of this fusion construct, suggesting that SUMO modification is a major rate-limiting step. This correlates with our observation that NF-κB activation in response to genotoxic stress is augmented in PIDD-expressing cells and attains its maximum level of activation more rapidly (Figure 2C), an effect that is most likely due to increased NEMO-SUMO levels. The effect of PIDD siRNA treatment on the modification of NEMO appears to be stronger than its effect on NF-κB activation, leaving the possibility open that there are other redundant pathways operational that lead to genotoxic-stress-induced NF-κB activation.

Given the complexity of sumoylation reactions, we can envisage several mechanisms that could explain the enhanced

Figure 3. PIDD Induces Modification of NEMO

(A) PIDD-expressing cells show an enhanced modification of NEMO upon induction of genotoxic stress. HEK293T cells stably expressing EV (mock) or PIDD were stimulated for the indicated time periods with 40 μM etoposide or 2 μg/ml doxorubicin. Lysates were analyzed for the presence of NEMO by Western blotting with a mouse anti-NEMO antibody.

(B) NEMO sumoylation and ubiquitination are induced in DNA-damage-treated PIDD-expressing cells. HEK293T mock or PIDD stably expressing cells were stimulated for 2 hr with 10 ng/ml TNF or 40 μM etoposide. Lysates were prepared in RIPA/SDS buffer to avoid coimmunoprecipitation of interacting proteins, immunoprecipitated with a rabbit anti-NEMO antibody, and evaluated for the presence of SUMO-1 and ubiquitin modification of NEMO.

(C) PIDD is essential for genotoxic-stress-induced SUMO modification and phosphorylation of NEMO. HEK293T cells were transfected with siRNA constructs targeting RAIDD, PIDD, or a scrambled control and stimulated with etoposide or doxorubicin or left untreated. NP40 lysates were immunoprecipitated with a rabbit anti-NEMO antibody and evaluated by Western blotting with a mouse anti-NEMO antibody for detection of SUMO-modified or phosphorylated NEMO species. Three different exposure times of the same blot are shown. Total cell lysates were also analyzed for phosphorylation of IκB. * corresponds to NEMO species from a previous exposure and was used as a loading control.

(D) PIDD is essential for genotoxic-stress-induced ubiquitination of NEMO. HEK293T cells were transfected with siRNA constructs targeting RAIDD, PIDD, or a scrambled control and stimulated with doxorubicin or left untreated. RIPA lysates were immunoprecipitated with a rabbit anti-NEMO antibody and evaluated by Western blotting with anti-ubiquitin antibody for detection of modified NEMO species.

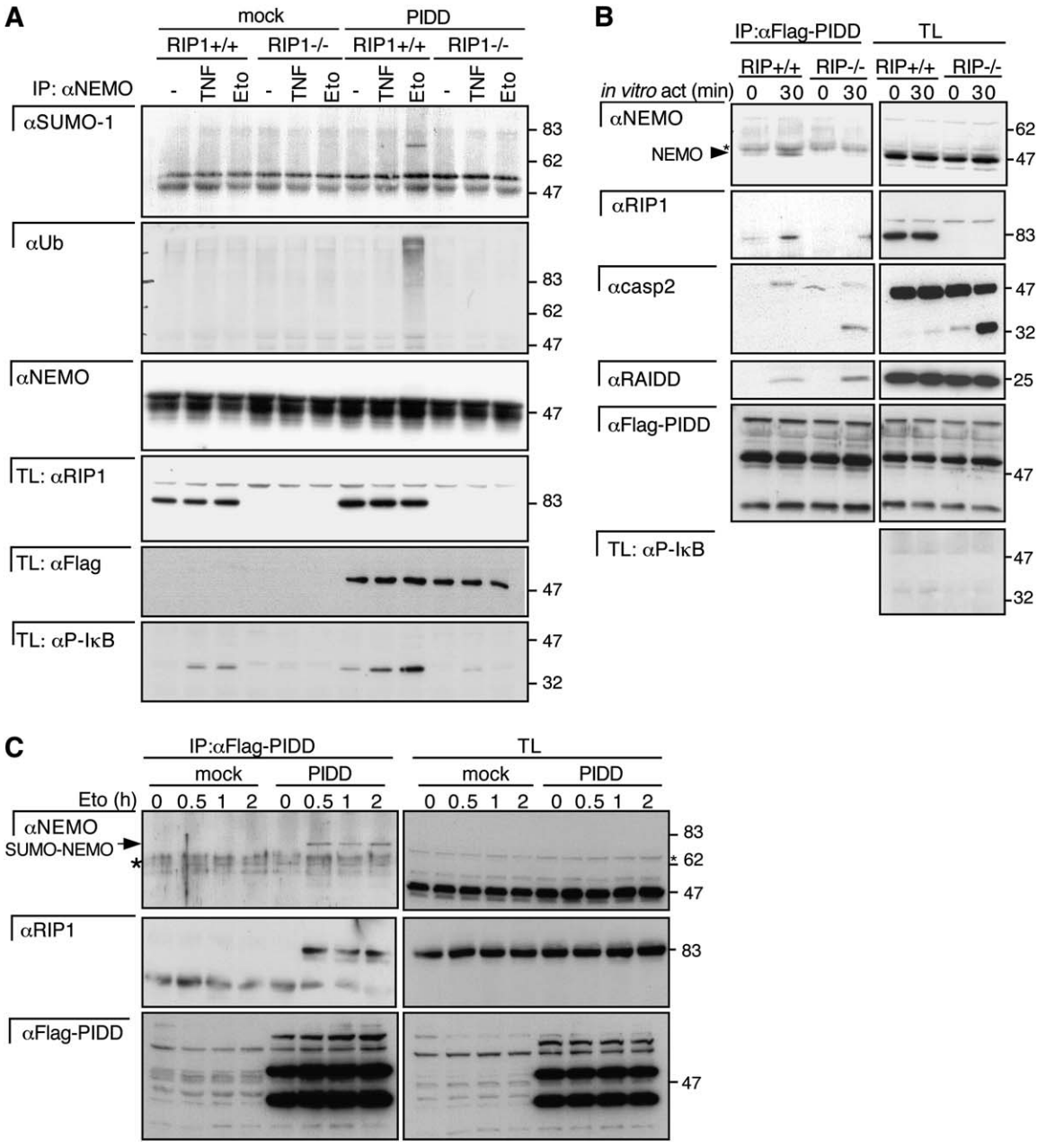

Figure 4. RIP1 Is Required to Establish a Complex, Induced upon Genotoxic Stress, between PIDD and NEMO

(A) PIDD-enhanced modification of NEMO upon treatment with genotoxic stress is strictly dependent on the presence of RIP1. RIP1-wt (*RIP1*$^{+/+}$) or RIP1-deficient (*RIP1*$^{-/-}$) Jurkat cells, either mock or PIDD transfected, were left untreated or stimulated for 2 hr with 10 ng/ml TNF or 40 μM etoposide. Lysates were prepared in RIPA/SDS buffer to avoid coimmunoprecipitation of interacting proteins, immunoprecipitated with a rabbit anti-NEMO, and evaluated for the presence of SUMO-1 and ubiquitin modification of NEMO. Total cell extracts (TL) were also analyzed for phospho-IκB.

(B) RIP1-wt (*RIP1*$^{+/+}$) or RIP1-deficient (*RIP1*$^{-/-}$) Jurkat cells stably expressing Flag-PIDD were lysed under hypotonic conditions and incubated for the indicated times at 37°C to allow spontaneous formation of the PIDDosome complex. Anti-Flag-PIDD immunoprecipitates were analyzed for the presence of NEMO, RIP1, caspase-2, RAIDD, or Flag-PIDD by Western blot. Total cell extracts (TL) were analyzed for phospho-IκB as well. *represents the heavy chain of IgG.

(C) PIDD, RIP1, and NEMO form a complex induced by genotoxic stress. HEK293T mock-transfected or PIDD-expressing cells were stimulated for the indicated times with 40 μM etoposide. Anti-Flag-PIDD immunoprecipitates were analyzed for the presence of NEMO and RIP1 by Western blot. *represents an unspecific band recognized by the rabbit anti-NEMO antibody.

sumoylation of NEMO. PIDD may recruit a known or an as yet unknown E3 ligase to NEMO, leading to its enhanced sumoylation. Alternatively, PIDD could act as an E3 ligase itself and directly enhance sumoylation of NEMO. This possibility is less likely, however, as NEMO is not modified when incorporated in the in vitro-assembled PIDDosome, suggesting

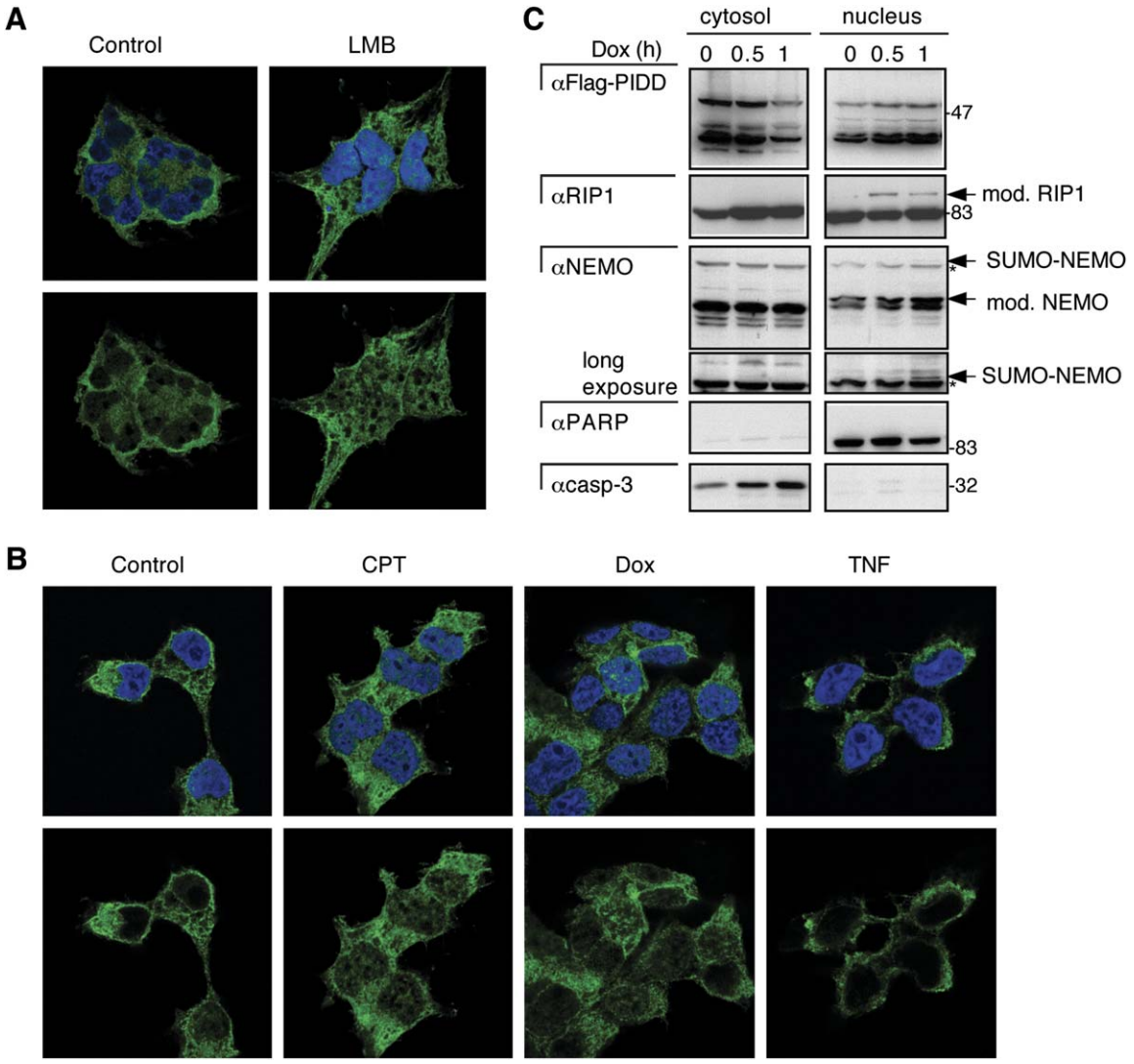

Figure 5. PIDD Translocates to the Nucleus in Response to Genotoxic Stress

(A) PIDD-expressing HEK293T cells were left untreated or were stimulated for 2 hr with leptomycin B (LMB). Confocal images show nuclear (blue, DRAQ5) or PIDD (green, Alexa 488) staining.

(B) PIDD-expressing HEK293T cells were left untreated or were stimulated for 2 hr with 50 μM CPT, 2 μg/ml doxorubicin, or 10 ng/ml TNF. Confocal images show nuclear (blue, DRAQ5) or PIDD (green, Alexa 488) staining.

(C) PIDD-expressing HEK293T cells were stimulated for the indicated time periods with 2 μg/ml doxorubicin. Cytosolic and nuclear fractions were prepared, verified for purity by analyzing PARP and caspase-3 levels, and evaluated for the presence of Flag-PIDD, RIP1, and NEMO. *represents an unspecific band recognized by the rabbit anti-NEMO antibody.

that additional components, activated upon genotoxic stress, are required. Another attractive possibility is that PIDD could stabilize SUMO-modified NEMO from desumoylation, akin to SUMO-modified RanGAP1, which is resistant to SENP2 (a SUMO isopeptidase) only when complexed with both RanBP2 and Ubc9 (Pichler and Melchior, 2002; Zhang et al., 2002). As RanBP2 does not act as an E3 ligase for RanGAP1, its SUMO-enhancing activity on RanGAP1 is thought to be solely due to this stabilizing function (Pichler and Melchior, 2002).

In addition to PIDD, RIP1 appears to play an essential role in DNA-damage-induced NF-κB activation. RIP1 is known to be recruited to the TNF-R1 signaling complex and to be indispensable for NF-κB activation by TNF (Kelliher et al., 1998). This raises the possibility that DNA-damage-induced NF-κB occurs through activation of the TNF-R1 signaling cascade. However, DNA-damage-induced NF-κB activation is unaltered in TNF-R1-deficient cells (Hur et al., 2003), and NEMO sumoylation is not observed in TNF-induced NF-κB activation (Figure 3B), indicating that RIP1 is also implicated in pathways in addition to that triggered by TNF. Based on our data, it is very likely that PIDD is positioned upstream of RIP1 in the signaling cascade triggered by genotoxic stress. Similar to TNF-R1, PIDD contains a DD that binds

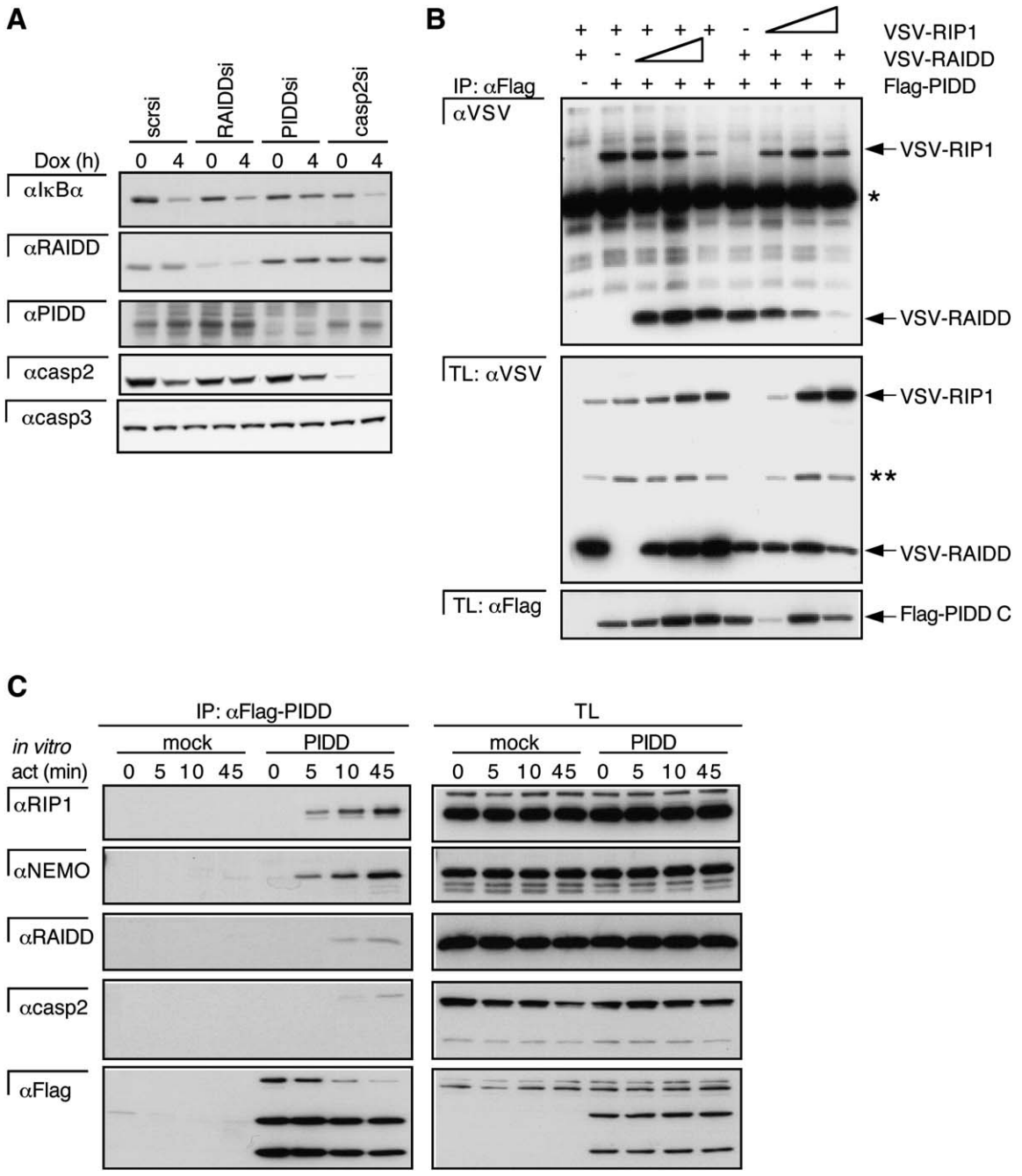

Figure 6. PIDD-Induced NF-κB and Apoptosis Pathways Are Independent

(A) RAIDD and caspase-2 are not essential for genotoxic-stress-induced NF-κB activation. U2OS cells were transfected with siRNA constructs targeting RAIDD, PIDD, caspase-2, or a scrambled control and, 48 hr after transfection, were stimulated with 2 μg/ml doxorubicin for 2 hr. Cell lysates were evaluated for IκB degradation by Western blot analysis. Caspase-3 was used as a loading control.

(B) RAIDD and RIP1 compete for binding to PIDD. HEK293T cells were transiently transfected with fixed amounts of expression vectors encoding Flag-PIDD and VSV-RIP1 and increasing amounts of VSV-RAIDD or vice versa. PIDD was immunoprecipitated from the lysates with anti-Flag antibodies, and coimmunoprecipitating proteins were revealed by Western blotting. *corresponds to the IgG1 heavy-chain band. **indicates degradation product of RIP1.

(C) RAIDD and RIP1 are recruited to activated PIDD with different kinetics. HEK293T cells stably expressing Flag-PIDD were lysed under hypotonic conditions and incubated for the indicated times at 37°C, which leads to spontaneous formation of the PIDDosome complex. Anti-Flag-PIDD immunoprecipitates were analyzed for the presence of RAIDD and RIP1 by Western blotting.

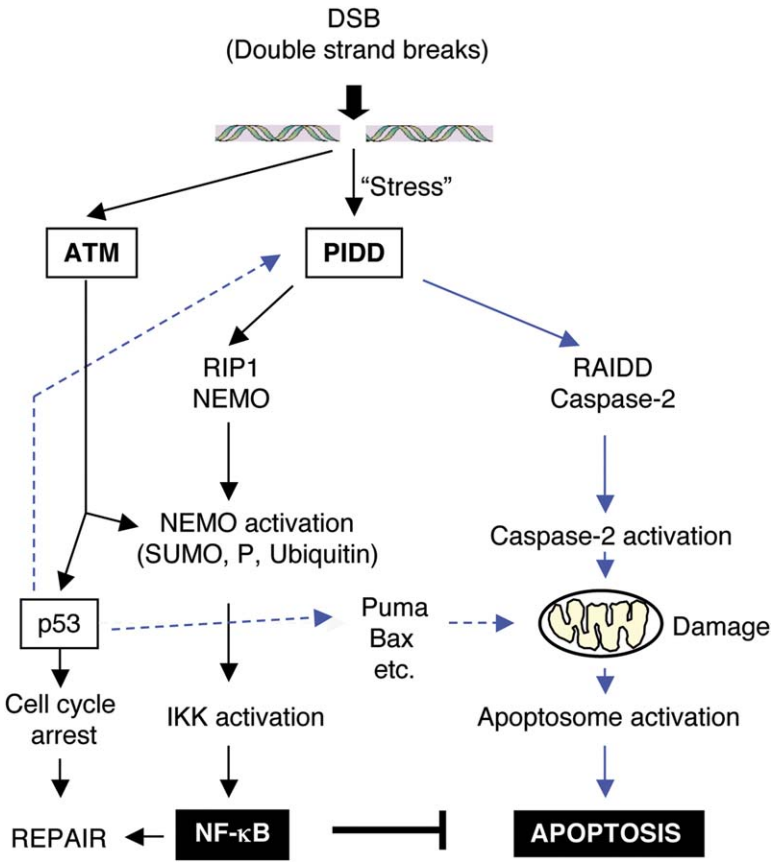

Figure 7. PIDD Acts as a Molecular Switch, Controlling the Balance between Life and Death upon DNA Damage
See text for details.

to the DD of RIP1 (data not shown). In both signaling pathways, RIP1 is subsequently modified. While RIP1 is ubiquitinated following treatment with TNF (Legler et al., 2003), the modification of RIP1 caused by genotoxic stress (Figure 5C) is currently unknown. RIP1 recruitment is required for PIDD-NEMO binding and modification, ultimately leading to the activation of IKKs. In both pathways, ubiquitination of NEMO appears to be a pivotal event for the activation of the IKK signalosome (Huang et al., 2003; Tang et al., 2003). Both pathways, however, are clearly distinct with respect to the site of assembly. The TNF-R1 complex is formed at the cell membrane, while data currently available suggest assembly of the PIDDosome in the nucleus. We observed that a small portion of the mostly cytoplasmic PIDD accumulates in the nucleus upon DNA damage, where it can encounter RIP1 and NEMO that both appear to be evenly distributed in the cytosolic and nuclear compartment.

The question arises as to how DNA damage is sensed by PIDD, leading to complex formation. Based on the capacity of LRRs to detect pathogen-associated molecular patterns in various Toll-like receptors, it is very likely that the LRRs of PIDD are implicated in binding directly or indirectly to a protein that is activated in DNA-damaged cells. As the PIDDosome spontaneously assembles in cell extracts, this presumptive ''signaling molecule'' is likely to be activated as well or exposed upon cell rupture. The future identification of this molecule will contribute greatly to our understanding of DNA-damage-induced stress.

In addition to RIP1 and NEMO, PIDD also complexes with RAIDD and caspase-2. As our results show, the NF-κB and apoptotic machineries are recruited to PIDD in a sequential manner (early recruitment of RIP1-NEMO versus late recruitment of RAIDD-caspase-2). Evidence for the existence of two distinct signaling platforms comes from competition experiments showing that RIP1 and RAIDD interact in a mutually exclusive manner with PIDD. Moreover, in cells lacking RIP1, kinetics of caspase-2 activation is highly accelerated (Figure 4C), suggesting that an active NF-κB pathway blocks or delays the caspase-2-mediated death pathway. Finally, siRNA against RAIDD or caspase-2 showed that these two molecules are dispensable for genotoxic-stress-induced NF-κB activation.

Although many questions concerning the PIDD-RIP1-NEMO signaling pathway remain open, the following model could explain how the PIDDosome might integrate DNA-damage signals (Figure 7). In unstimulated cells, PIDD is mainly cytoplasmic. Upon genotoxic stress, PIDD detects a stress-related signal of currently unknown nature, which causes its nuclear translocation and/or retention, allowing PIDD to accumulate in the nucleus and interact with RIP1 and NEMO, both of which are already present in the nucleus. NEMO sumoylation and RIP1 modification then ensue. In parallel, genotoxic stress induces activation of the protein kinase ATM, which phosphorylates sumoylated NEMO, leading to ubiquitination, nuclear export of NEMO, and subsequent IKK activation in the cytoplasm. As amply

documented, the majority of the substrates activated by ATM are implicated in cell-cycle control and activation of the p53 pathway or in DNA repair (Shiloh, 2003). Together, these ATM-activated pathways allow the cell to repair damage and restore normal growth unharmed. However, this may not be always possible, and, in cases of excessive DNA damage, an apoptotic program is induced to avoid possible cellular transformation. In addition to PIDD, DNA-damage-induced p53 transcriptional activity also leads to the induction of several proapoptotic genes such as Bax, Puma, or Noxa (Nakano and Vousden, 2001; Slee et al., 2004; Villunger et al., 2003). De novo gene transcription of PIDD and consequent activation of caspase-2, together with the activation of the other p53-dependent proapoptotic genes, eventually lead to the execution phase in which the cell activates its own suicide program. This model predicts that knockdown of PIDD will not ablate p53-induced apoptosis, considering that the BH3 members Noxa or Puma can induce mitochondrial damage independently of caspase-2. Indeed, we found that reduced PIDD levels slightly increase the sensitivity of cells to genotoxic-stress-induced apoptosis, which can be explained by decreased NF-κB activity (Figure S3C). Just like p53, PIDD thus acts as a molecular switch, able to activate a survival or apoptotic program. The final outcome is probably determined by the type and amount of damage to the genome and the overall physiological state of the cell.

EXPERIMENTAL PROCEDURES

Cell Culture and Biological Reagents

Human embryonic kidney (HEK) cells, U2OS human osteosarcoma cells, HeLa cells, and HEK293T cells stably expressing PIDD were grown in DMEM and Glutamax (Life Technologies) supplemented with 10% fetal calf serum and 100 U/ml penicillin, 100 μg/ml streptomycin. RIP1-wt and RIP1-deficient Jurkat cells were grown in RPMI containing Glutamax (Life Technologies) supplemented with 10% fetal calf serum and 100 U/ml penicillin, 100 μg/ml streptomycin. The generation of cells stably expressing PIDD was described elsewhere (Tinel and Tschopp, 2004). Cells stably expressing PIDD were always compared to mock-transfected cells (transfected with empty vector). Camptothecin, human recombinant TNFα, and etoposide were purchased from Alexis. Doxorubicin was obtained from Sigma.

Expression Vectors

pCR3-PIDD-Flag, pMSCV-PIDD-Flag, pCR3-RAIDD-Flag, pCR3-caspase-2-Flag, pCR3-RIP1-Flag, pCR3-RAIDD-VSV, and pCR3-RIP1-VSV have been described previously (Tinel and Tschopp, 2004). pNFconluc, containing the luciferase reporter gene driven by a minimal NF-κB-responsive promoter, was a gift of Dr. A. Israel (Institut Pasteur, Paris). pactβgal, containing the β-galactosidase gene under the control of the β-actin promoter, was obtained from Dr. T. Inoue (Institute of Medical Sciences, Tokyo).

Transient Transfections and NF-κB Reporter Gene Assays

HEK293T and HEK293 cells stably expressing PIDD or the empty vector were transiently transfected by the DNA-calcium-phosphate precipitation method with 100 ng pNFconluc, 100 ng pactβgal, and different concentrations of specific expression plasmids. The total amount of DNA was kept constant by adding empty vector up to 1 μg DNA per six-well. NF-κB activity was determined by measuring the luciferase activity present in cell extracts. Luciferase values were normalized for differences in transfection efficiency on the basis of β-galactosidase activity in the same extracts and expressed as fold induction values relative to the unstimulated empty-vector control. Where needed, cells were stimulated 48 hr post-transfection for 16 hr with 2 μg/ml doxorubicin, 40 μM etoposide, 50 μM camptothecin or left untreated.

Preparation and Transfection of siRNA

siRNA oligonucleotides against RAIDD (GGCCAGAGACAAACAAG TACTC), PIDD (CAGACTGTTCCTGACCTCAGA), and caspase-2 (AAA CAGCTGTTGTTGAGCGAA) were purchased from QIAGEN. siRNA oligonucleotides against RIP1 (GGCGAAGATGATGAACAGA) were obtained from Ambion. A scrambled siRNA was used with sequence GGTTCTTCAGTACCTCTACCA. HEK293T cells were transfected using the calcium-phosphate precipitation technique. U2OS cells were transfected using Oligofectamin (Invitrogen).

EMSA Assays

HEK293T cells were transfected with a siRNA control or a siRNA construct targeting PIDD. Forty-eight hours after transfection, cells were stimulated for different time periods with 40 μM etoposide. Nuclear fractions were prepared as described elsewhere (Petrilli et al., 2004). ^{32}P-labeled double-stranded oligonucleotides containing the κB site from the Igκ gene were prepared as described by Miyamoto et al. (1994) (wt, 5′-TCAA CAGAGGGGACTTTCCGAGAGGCC-3′; mutated, 5′-TCAACAGAG CTCACTTTATGAGAGGCC-3′). DNA/nucleoprotein complexes were separated from free probe on a 4% polyacrylamide gel.

RT-PCR

U2OS cells were transfected with a scrambled siRNA or siRNA against PIDD. Forty-eight hours later, cells were treated for different time periods with 40 μM etoposide. RNA was prepared with Trizol (Invitrogen), and 5 μg was used for a T-primed RT-PCR reaction (Amersham). Specific primers were used to amplify actin, XIAP (sense, TGGCAATATGGAGACT CAGC; antisense, TGCACTTGGTCACCAATACC), or Bcl-xL (sense, CATGGCAGCAGTAAAGCAAGCG; antisense, AGGCTCTAGGTGGTCA TTCAGG).

In Vitro Activation and Immunoprecipitation

Preparation of the lysates in hypotonic buffer and in vitro activation and immunoprecipitation were performed as described previously (Tinel and Tschopp, 2004). Cells were washed twice with PBS and resuspended in hypotonic buffer (20 mM HEPES-KOH, 10 mM KCl, 1 mM $MgCl_2$, 1 mM EDTA, 1 mM EGTA, 1 mM DTT [pH 7.5]) supplemented with protease inhibitors (Complete, Roche). Resuspended cells were lysed by using a 22G needle. Cellular debris was removed by centrifugation at 10,000 × g for 20 min at 4ºC followed by filtration at 0.4 μm. Clear lysates were incubated at 37ºC for the indicated times or left untreated on ice. After incubation, an equivalent volume of hypotonic buffer containing 0.1% NP-40 and 300 mM NaCl was added. The mix was incubated overnight with M2-Flag beads (Sigma) at 4ºC on a rotating wheel.

Coimmunoprecipitation and Western Blotting

PIDD complexes were revealed after either in vitro activation for the indicated times of lysates of PIDD-expressing cells and immunoprecipitation of Flag-PIDD (see description before) or after activation of the cells by treatment with 40 μM etoposide for different periods. Lysates were prepared in E1A lysis buffer (1% NP-40, 20 mM HEPES [pH 7.9], 250 mM NaCl, 20 mM β-glycerophosphate, 10 mM NaF, 1 mM sodium orthovanadate, 2 mM dithiothreitol, 1 mM EDTA, and a protease-inhibitor cocktail), and Flag-PIDD was immunoprecipitated from cleared lysates with M2-Flag beads (Sigma) at 4ºC on a rotating wheel. Sumoylated or ubiquitinated forms of NEMO were detected by preparing lysates of stimulated cells in RIPA buffer (25 mM Tris [pH 8.2], 50 mM NaCl, 0.5% NP-40, 0.5% deoxycholic acid, 0.1% SDS, 10 mM iodoacetate) supplemented with protease and phosphatase inhibitors and sheared using a 22G needle. Cleared lysates were incubated overnight with a rabbit NEMO antibody that was preincubated with protein G Sepharose. Coimmunoprecipitation experiments with transfected proteins were done in E1A lysis buffer. After lysis, the extracts were incubated with anti-Flag beads for

2 hr. After incubation, the beads were washed six times with lysis buffer, separated by SDS-PAGE, transferred to nitrocellulose, and analyzed by immunoblotting. Antibodies used were anti-IκB (Santa Cruz), anti-phospho-IκB (Cell Signaling), rabbit anti-NEMO (Santa Cruz), mouse anti-NEMO (Transduction Labs), anti-RIP1 (Transduction Labs), anti-FADD (Transduction Labs), anti-TRAF6 (Santa Cruz), anti-RAIDD (MBL), anti-RIP2 (Alexis), anti-caspase-2 11B4 (Apotech), anti-SUMO-1 (Zymed), anti-ubiquitin (Santa Cruz), anti-Flag and anti-VSV (Sigma), anti-ATM (Genetex), anti-P-ATM (Cell Signaling), anti-caspase-3 (Transduction Labs), and anti-PARP (Cell Signaling). AL233 is a rabbit polyclonal antibody raised against PIDD-DD (776–910) by Eurogentec. 1G3-4F7 is a monoclonal PIDD antibody raised against PIDD-DD (776–910).

Biochemical Fractionation

HEK293T cells stably expressing PIDD were treated with 2 μg/ml doxorubicin for different time periods. Cytoplasmic and nuclear fractions were prepared according to the protocol of Dignam et al. (1983). Briefly, cells were lysed in a cytosolic lysis buffer containing 10 mM HEPES (pH 7.9), 1.5 mM $MgCl_2$, 300 mM sucrose, 0.5% NP-40, 10 mM KCl supplemented with DTT and protease inhibitors. Nuclei were pelleted by a short centrifugation and lysed in a nuclear buffer containing 20 mM HEPES (pH 7.9), 100 mM NaCl, 0.2 mM EDTA, 20% glycerol, 100 mM KCl supplemented with DTT and protease inhibitors. Nuclear pellets were subjected to a freeze-thaw cycle, sonicated, and centrifuged to obtain a solubilized nuclear fraction.

Immunostaining and Confocal Microscopy

PIDD stable HEK293T or EV cells were cultured on sterile glass coverslips in six-well plates and fixed with a solution containing 1% paraformaldehyde, 2% glucose, and 5 mM azide in PBS for 15 min. Cells were permeabilized with 0.3% saponin for 10 min and treated with 2% normal goat serum (NGS)/0.5% BSA/0.1% saponin as a blocking reagent. Flag antibody (M2, Sigma) was used at a dilution of 1/500 in 0.1% saponin/0.1% BSA/PBS, while a secondary Alexa 488 anti-mouse IgG1 (Molecular Probes) was used at a dilution of 1/300 in 0.1% saponin/0.1% BSA/PBS. Cells were mounted in FluorSave (Calbiochem) containing a 1/1000 dilution of DRAQ5 (Alexis) for nuclear counterstain. Images from immunostaining were collected by using a Zeiss inverted laser scanning confocal microscope LSM 510 with a 63× oil immersion objective.

Supplemental Data

Supplemental Data include three figures and can be found with this article online at http://www.cell.com/cgi/content/full/123/6/1079/DC1/.

ACKNOWLEDGMENTS

We would like to thank Natalia Olivos and Nadège Roduit for excellent technical assistance, Helen Everett for comments and critical reading of the manuscript, and all members of the laboratory for helpful discussions and comments. S.J. is the recipient of an EMBO long-term fellowship.

Received: April 12, 2005
Revised: July 19, 2005
Accepted: September 12, 2005
Published: December 15, 2005

REFERENCES

Avemann, K., Knippers, R., Koller, T., and Sogo, J.M. (1988). Camptothecin, a specific inhibitor of type I DNA topoisomerase, induces DNA breakage at replication forks. Mol. Cell. Biol. *8*, 3026–3034.

Baldwin, A.S. (2001). Control of oncogenesis and cancer therapy resistance by the transcription factor NF-kappaB. J. Clin. Invest. *107*, 241–246.

Boland, M.P., Fitzgerald, K.A., and O'Neill, L.A. (2000). Topoisomerase II is required for mitoxantrone to signal nuclear factor kappa B activation in HL60 cells. J. Biol. Chem. *275*, 25231–25238.

Bonizzi, G., and Karin, M. (2004). The two NF-kappaB activation pathways and their role in innate and adaptive immunity. Trends Immunol. *25*, 280–288.

Bromberg, K.D., Burgin, A.B., and Osheroff, N. (2003). A two-drug model for etoposide action against human topoisomerase IIalpha. J. Biol. Chem. *278*, 7406–7412.

Burns, K.A., and Martinon, F. (2004). Inflammatory diseases: is ubiquitinated NEMO at the hub? Curr. Biol. *14*, R1040–R1042.

Campbell, K.J., Rocha, S., and Perkins, N.D. (2004). Active repression of antiapoptotic gene expression by RelA(p65) NF-kappa B. Mol. Cell *13*, 853–865.

Dignam, J.D., Lebovitz, R.M., and Roeder, R.G. (1983). Accurate transcription initiation by RNA polymerase II in a soluble extract from isolated mammalian nuclei. Nucleic Acids Res. *11*, 1475–1489.

Endter, C., Kzhyshkowska, J., Stauber, R., and Dobner, T. (2001). SUMO-1 modification required for transformation by adenovirus type 5 early region 1B 55-kDa oncoprotein. Proc. Natl. Acad. Sci. USA *98*, 11312–11317.

Fukuda, M., Asano, S., Nakamura, T., Adachi, M., Yoshida, M., Yanagida, M., and Nishida, E. (1997). CRM1 is responsible for intracellular transport mediated by the nuclear export signal. Nature *390*, 308–311.

Hay, R.T. (2004). Modifying NEMO. Nat. Cell Biol. *6*, 89–91.

Hay, R.T. (2005). SUMO: a history of modification. Mol. Cell *18*, 1–12.

Hayden, M.S., and Ghosh, S. (2004). Signaling to NF-kappaB. Genes Dev. *18*, 2195–2224.

Huang, T.T., Wuerzberger-Davis, S.M., Seufzer, B.J., Shumway, S.D., Kurama, T., Boothman, D.A., and Miyamoto, S. (2000). NF-kappaB activation by camptothecin. A linkage between nuclear DNA damage and cytoplasmic signaling events. J. Biol. Chem. *275*, 9501–9509.

Huang, T.T., Wuerzberger-Davis, S.M., Wu, Z.H., and Miyamoto, S. (2003). Sequential modification of NEMO/IKKgamma by SUMO-1 and ubiquitin mediates NF-kappaB activation by genotoxic stress. Cell *115*, 565–576.

Hur, G.M., Lewis, J., Yang, Q., Lin, Y., Nakano, H., Nedospasov, S., and Liu, Z.G. (2003). The death domain kinase RIP has an essential role in DNA damage-induced NF-kappa B activation. Genes Dev. *17*, 873–882.

Johnson, E.S., and Gupta, A.A. (2001). An E3-like factor that promotes SUMO conjugation to the yeast septins. Cell *106*, 735–744.

Jung, M., Kondratyev, A., Lee, S.A., Dimtchev, A., and Dritschilo, A. (1997). ATM gene product phosphorylates I kappa B-alpha. Cancer Res. *57*, 24–27.

Kagey, M.H., Melhuish, T.A., and Wotton, D. (2003). The polycomb protein Pc2 is a SUMO E3. Cell *113*, 127–137.

Kato, T., Jr., Delhase, M., Hoffmann, A., and Karin, M. (2003). CK2 Is a C-Terminal IkappaB Kinase Responsible for NF-kappaB Activation during the UV Response. Mol. Cell *12*, 829–839.

Kelliher, M.A., Grimm, S., Ishida, Y., Kuo, F., Stanger, B.Z., and Leder, P. (1998). The death domain kinase RIP mediates the TNF-induced NF-kappaB signal. Immunity *8*, 297–303.

Lamkanfi, M., D'Hondt, K., Vande Walle, L., van Gurp, M., Denecker, G., Demeulemeester, J., Kalai, M., Declercq, W., Saelens, X., and Vandenabeele, P. (2005). A novel caspase-2 complex containing TRAF2 and RIP1. J. Biol. Chem. *280*, 6923–6932.

Legler, D.F., Micheau, O., Doucey, M.A., Tschopp, J., and Bron, C. (2003). Recruitment of TNF receptor 1 to lipid rafts is essential for TNFalpha-mediated NF-kappaB activation. Immunity *18*, 655–664.

Li, N., Banin, S., Ouyang, H., Li, G.C., Courtois, G., Shiloh, Y., Karin, M., and Rotman, G. (2001). ATM is required for IkappaB kinase (IKKk) activation in response to DNA double strand breaks. J. Biol. Chem. *276*, 8898–8903.

Li, X., Zhang, R., Luo, D., Park, S.J., Wang, Q., Kim, Y., and Min, W. (2005). Tumor necrosis factor alpha-induced desumoylation and cytoplasmic translocation of homeodomain-interacting protein kinase 1 are

critical for apoptosis signal-regulating kinase 1-JNK/p38 activation. J. Biol. Chem. *280*, 15061–15070. Published online February 8, 2005. 10.1074/jbc.M414262200.

Lin, Y., Ma, W., and Benchimol, S. (2000). Pidd, a new death-domain-containing protein, is induced by p53 and promotes apoptosis. Nat. Genet. *26*, 122–127.

Meylan, E., and Tschopp, J. (2005). The RIP kinases: crucial integrators of cellular stress. Trends Biochem. Sci. *30*, 151–159.

Miyamoto, S., Schmitt, M.J., and Verma, I.M. (1994). Qualitative changes in the subunit composition of kappa B-binding complexes during murine B-cell differentiation. Proc. Natl. Acad. Sci. USA *91*, 5056–5060.

Nakano, K., and Vousden, K.H. (2001). PUMA, a novel proapoptotic gene, is induced by p53. Mol. Cell *7*, 683–694.

Pahl, H.L. (1999). Activators and target genes of Rel/NF-kappaB transcription factors. Oncogene *18*, 6853–6866.

Petrilli, V., Herceg, Z., Hassa, P.O., Patel, N.S., Di Paola, R., Cortes, U., Dugo, L., Filipe, H.M., Thiemermann, C., Hottiger, M.O., et al. (2004). Noncleavable poly(ADP-ribose) polymerase-1 regulates the inflammation response in mice. J. Clin. Invest. *114*, 1072–1081.

Pichler, A., and Melchior, F. (2002). Ubiquitin-related modifier SUMO1 and nucleocytoplasmic transport. Traffic *3*, 381–387.

Pichler, A., Gast, A., Seeler, J.S., Dejean, A., and Melchior, F. (2002). The nucleoporin RanBP2 has SUMO1 E3 ligase activity. Cell *108*, 109–120.

Piret, B., Schoonbroodt, S., and Piette, J. (1999). The ATM protein is required for sustained activation of NF-kappaB following DNA damage. Oncogene *18*, 2261–2271.

Rangasamy, D., Woytek, K., Khan, S.A., and Wilson, V.G. (2000). SUMO-1 modification of bovine papillomavirus E1 protein is required for intranuclear accumulation. J. Biol. Chem. *275*, 37999–38004.

Read, S.H., Baliga, B.C., Ekert, P.G., Vaux, D.L., and Kumar, S. (2002). A novel Apaf-1-independent putative caspase-2 activation complex. J. Cell Biol. *159*, 739–745.

Seeler, J.S., and Dejean, A. (2003). Nuclear and unclear functions of SUMO. Nat. Rev. Mol. Cell Biol. *4*, 690–699.

Shiloh, Y. (2003). ATM and related protein kinases: safeguarding genome integrity. Nat. Rev. Cancer *3*, 155–168.

Slee, E.A., O'Connor, D.J., and Lu, X. (2004). To die or not to die: how does p53 decide? Oncogene *23*, 2809–2818.

Tang, E.D., Wang, C.Y., Xiong, Y., and Guan, K.L. (2003). A role for NF-kappaB essential modifier/IkappaB kinase-gamma (NEMO/IKKgamma) ubiquitination in the activation of the IkappaB kinase complex by tumor necrosis factor-alpha. J. Biol. Chem. *278*, 37297–37305.

Telliez, J.B., Bean, K.M., and Lin, L.L. (2000). LRDD, a novel leucine rich repeat and death domain containing protein. Biochim. Biophys. Acta *1478*, 280–288.

Tewey, K.M., Rowe, T.C., Yang, L., Halligan, B.D., and Liu, L.F. (1984). Adriamycin-induced DNA damage mediated by mammalian DNA topoisomerase II. Science *226*, 466–468.

Tinel, A., and Tschopp, J. (2004). The PIDDosome, a protein complex implicated in activation of caspase-2 in response to genotoxic stress. Science *304*, 843–846.

Villunger, A., Michalak, E.M., Coultas, L., Mullauer, F., Bock, G., Ausserlechner, M.J., Adams, J.M., and Strasser, A. (2003). p53- and drug-induced apoptotic responses mediated by BH3-only proteins puma and noxa. Science *302*, 1036–1038.

Zhang, H., Saitoh, H., and Matunis, M.J. (2002). Enzymes of the SUMO modification pathway localize to filaments of the nuclear pore complex. Mol. Cell. Biol. *22*, 6498–6508.